Screening of catalysts for acrylonitrile decomposition

Tetsuya Nanba*, Shoichi Masukawa, Junko Uchisawa, and Akira Obuchi

Institute for Environmental Management Technology, National Institute of Advanced Industrial Science and Technology (AIST), 16-1 Onogawa, Tsukuba, Ibaraki 305-8569, Japan

Received 12 August 2003; accepted 9 January 2004

The catalytic decomposition of acrylonitrile over various metal components (Mg, Ca, Mn, Fe, Co, Ni, Cu, Zn, Ga, Pd, Ag, and Pt) supported on several metal oxides (Al_2O_3, SiO_2, TiO_2, ZrO_2, and MgO) and ZSM-5 was studied. The most promising catalyst was Cu-ZSM-5, which exhibited 100% conversion and at least 80% N_2 selectivity above 350 °C.

KEY WORDS: acrylonitrile; decomposition; Cu-ZSM-5; Ag; TiO_2; ZrO_2.

1. Introduction

Among the nitrogen-containing volatile organic compounds (VOCs) that are emitted into the atmosphere, acrylonitrile (ACN) is of special concern because of its carcinogenicity [1]. In Japan, ACN is specified as one of 22 kinds of harmful pollutants for which primary efforts to prevent release into the atmosphere should be made. The half-life of ACN in the atmosphere is estimated to be 2–3 days, which is longer than that of formaldehyde or benzene. Since the threshold limit of ACN in work environments is as low as 2 ppm in the United States and Japan, a local exhaust gas treatment system is necessary in some cases.

Treatment of exhaust gas containing ACN and other VOCs by simple combustion is useful but requires a temperature above 850 °C [2]. Therefore, this process results in the secondary generation of NO_x ($NO + NO_2$) from atmospheric $N_2 + O_2$. Although a catalytic combustion system can treat exhaust gas at lower temperatures, nitrogen atoms in ACN lead to the formation of NO_x and other hazardous compounds [3]. Therefore, an ACN purification system that can convert ACN completely to harmless CO_2, H_2O, and N_2 needs to be developed.

In this study, we explored ACN decomposition catalysts by conducting activity screening tests for various metal and metal oxide based catalysts and found that Cu-ZSM-5 and several other catalysts are promising.

2. Experimental

2.1. Preparation of catalysts

The catalysts were prepared by the impregnation method. Precursors for the metal components were $Mg(NO_3)_2$ (Wako Pure Chemical Industries), $Ca(NO_3)_2$ (Wako Pure Chemical Industries), $Mn(CH_3COO)_2$ (Junsei Chemical), $Fe(NO_3)_3$ (Wako Pure Chemical Industries), $Co(NO_3)_3$ (Wako Pure Chemical Industries), $Ni(CH_3COO)_2$ (Nacalai Tesque), $Cu(NO_3)_2$ (Wako Pure Chemical Industries), $Zn(NO_3)_2$ (Junsei Chemical), $Ga(NO_3)_3$ (Kishida Chemical), $Pd(NO_3)_2$ (aqueous solution, Pd content = 8.5 wt%; N.E. Chemcat), $AgNO_3$ (Wako Pure Chemical Industries), and H_2PtCl_6 (Nacalai Tesque). The metal oxide supports were Al_2O_3 (KHS-46; Sumitomo Chemical, 170 m^2/g), SiO_2 (Wakogel C-100; Wako Pure Chemical Industries, 438 m^2/g), TiO_2 (P-25; Nippon-Aerosil, 67 m^2/g), ZrO_2 (RSC-H; Daiichi-Kigenso, 42 m^2/g), and MgO (Nacalai Tesque, 10 m^2/g). H-ZSM-5 zeolite was prepared by exchanging the Na ions of Na-ZSM-5 (HSZ-820-NAA, Tosoh) with the NH_4 ions of aqueous NH_4NO_3, and calcining the NH_4-ZSM-5 product at 773 K in air. The loading was adjusted to 5% as CaO, MgO, MnO_2, Fe_3O_4, CoO, NiO, Cu, ZnO, Ga_2O_3, and Ag, and 1% as Pt and Pd. Catalysts supported on ZSM-5 were prepared by ion exchange. The metal precursors were $Cu(CH_3COO)_2$ (Wako Pure Chemical Industries) and $AgNO_3$. Five grams of NH_4-ZSM-5 was suspended in 0.1 mol/L of the aqueous solution of the precursor, followed by washing with distilled water. All catalysts were calcined at 500 °C in air for 4 h.

2.2. Activity test

Activity tests were carried out at atmospheric pressure in a fixed-bed flow reactor, in which a quartz tube with 0.1 or 0.15 g of catalyst was placed. The flow rate of the reactant gas was 160 mL/min for 0.1 g of catalyst and 240 mL/min for 0.15 g of catalyst, which correspond to $W/F = 0.0375$ g s/mL. The reactant gas consisted of ca. 200 ppm ACN, 5% O_2, and 0 or 0.5% H_2O, with He as the balance gas. ACN was supplied to the reactant gas by passing a predetermined flow rate of

* To whom correspondence should be addressed.
E-mail: tty-namba@aist.go.jp

1011-372X/04/0300–0195/0 © 2004 Plenum Publishing Corporation

He through ACN liquid maintained at −18 °C. The products were analyzed as described elsewhere [4,5].

The catalytic activity was evaluated in terms of ACN conversion and selectivity of N_2, NO_x + N_2O (NO + NO_2 + N_2O), and other nitrogen-containing products (NCP):

$$\text{ACN conversion } (\%) = \frac{\text{Inlet ACN (ppm)} - \text{Outlet ACN (ppm)}}{\text{Inlet ACN (ppm)}} \times 100$$

$$\text{N}_2 \text{ selectivity } (\%) = \frac{\text{N}_2 \times 2(\text{ppm})}{\text{Total product N (ppm)}} \times 100$$

$$\text{NO}_x + \text{N}_2\text{O selectivity } (\%) = \frac{\text{N}_2\text{O} \times 2 + \text{NO}_x(\text{ppm})}{\text{Total product N (ppm)}} \times 100$$

$$\text{NCP selectivity } (\%) = \frac{\text{NCP (ppm)}}{\text{Total product N (ppm)}} \times 100$$

NO_x and N_2O were classified as undesirable nitrogen oxides. The NCPs detected were NH_3, HCN, HNCO, and acetonitrile. To ensure reliability, the selectivities were evaluated only when the ACN conversion was over 10%. No catalyst deactivation was observed under the activity test conditions applied in this study.

2.3. Characterization

The BET specific surface areas of the catalyst samples were measured by N_2 adsorption at −196 °C (Nikkisou, Model 4232). The metal loading of the ion-exchanged zeolites was measured by inductively coupled plasma emission spectroscopy (Seiko Electronics, SPS1200A). Temperature-programmed desorption of NH_3 (NH_3-TPD) was carried out with a TPD apparatus equipped with a mass spectrometer (Bel Japan Inc., TPD-1-AT). The TPD profiles were obtained over the range 100–600 °C in a 50 mL/min flow of He at a heating rate of 10 °C/min after adsorption of NH_3 at 100 °C. Temperature-programmed reduction (TPR) was carried out with a TPD apparatus equipped with a thermal conductivity detector (Ohkura-Riken, ADT700). The TPR profiles were obtained from room temperature to 600 °C in a 100 mL/min flow of 3% H_2/Ar at a heating rate of 10 °C/min after oxidation of the sample in a 5.25% O_2 flow at 500 °C for 2 h.

3. Results and discussion

3.1. Silica-supported catalysts

The activities and product selectivities of the silica-supported catalysts in table 1 are presented in figure 1. The activity is expressed as the temperature of 95% conversion of ACN (T_{95}), and the product selectivity is the product selectivity at this temperature. Since the SiO_2 support had negligible activity for ACN decomposition over the measured temperature range, the results in figure 1 are attributable to the activity of the metals or metal oxides on the SiO_2 support. Pt and Pd showed the highest ACN conversion activities, with T_{95} = ca. 250 °C. Mn, Co, Cu, and Ag had intermediate activities, and Fe and Ni had the lowest activities. The maximum ACN conversions on Mg, Ca, Zn, and Ga were only 53%, 25%, 14%, and 15% at 500 °C, respectively (not shown). Cu and Ag achieved the highest N_2 selectivities (68% and 61%, respectively). The Pt and Pd catalysts predominantly formed NO_x and N_2O, although they exhibited high ACN conversions.

Table 1
Physical property

Catalyst	Surface area (m^2/g)
Mg/SiO_2	399
Ca/SiO_2	324
Mn/SiO_2	390
Fe/SiO_2	412
Co/SiO_2	406
Ni/SiO_2	404
Zn/SiO_2	417
Cu/SiO_2	421
Ga/SiO_2	454
Pd/SiO_2	456
Ag/SiO_2	455
Pt/SiO_2	462
Cu/Al_2O_3	149
Cu/TiO_2	44
Cu/ZrO_2	35
Cu/MgO	19
Cu-ZSM-5[a]	293
Ag/Al_2O_3	172
Ag/TiO_2	36
Ag/ZrO_2	38
Ag/MgO	13
Ag-ZSM-5[b]	259

[a]Cu loading was 6.4 wt%.
[b]Ag loading was 7.4 wt%.

Table 1 lists the BET specific surface areas of the catalysts. Comparison of these values with the results in figure 1 shows that there is no relationship between the activity and the surface area.

Below, we focus on the Ag and Cu catalysts, which had the highest N_2 selectivity, with the aim of improving the ACN decomposition activity.

3.2. Ag catalysts

The ACN conversions and N_2 selectivity for the ACN + O_2 reaction on Ag supported on various materials are presented in figure 2. The ACN conversion depended on the support material, the order being Ag/ZrO_2 > Ag/MgO, Ag/SiO_2 > Ag/TiO_2 > Ag/Al_2O_3 > Ag-ZSM-5 (figure 2a). These catalysts can be divided into three categories according to their N_2 selectivity:

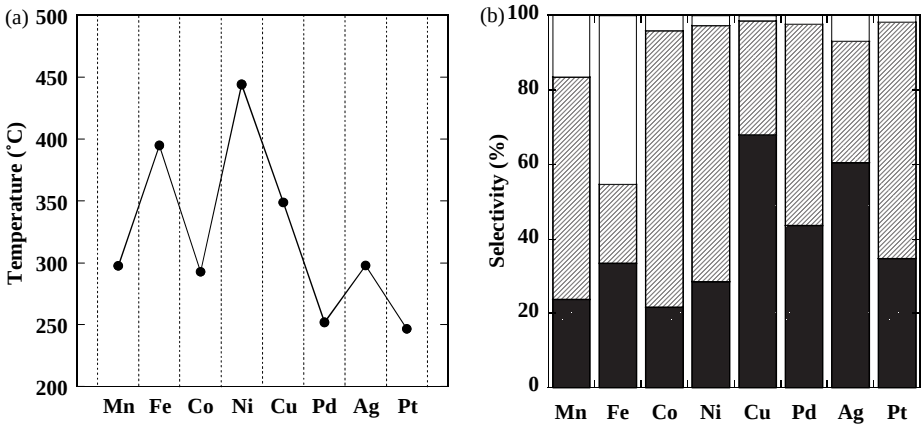

Figure 1. Temperature of 95% ACN conversion (T_{95}) (a) and product selectivity (b) in the ACN + O_2 reaction. $W/F = 0.0375$ g s/cm^3. The feed gas consisted of ca. 200 ppm ACN and 5% O_2. Shading patterns in (b) indicate selectivity to N_2 (heavy shading), NO_x + N_2O (light shading), and NCP (no shading).

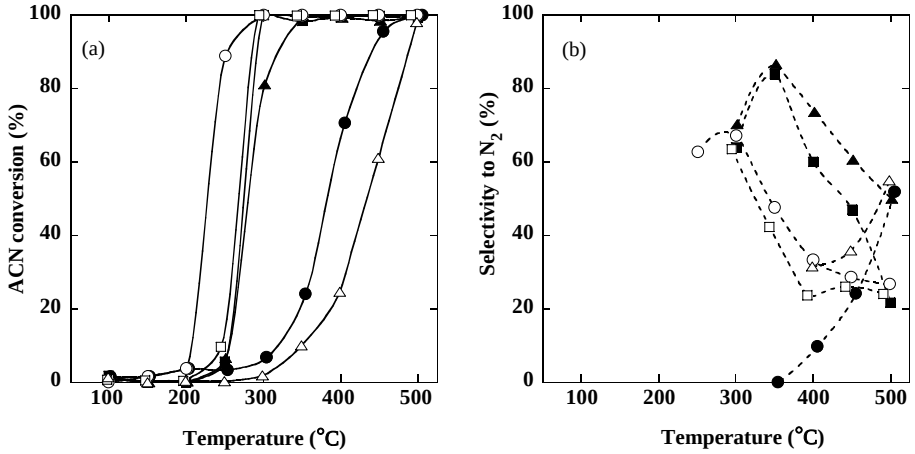

Figure 2. ACN conversion (a) and selectivity to N_2 (b) over Ag catalysts supported on various materials. $W/F = 0.0375$ g s/cm^3. The feed gas consisted of ca. 200 ppm ACN and 5% O_2. Symbols indicate Al_2O_3 (●), SiO_2 (■), TiO_2 (▲), ZrO_2 (○), MgO (□), and ZSM-5 (△).

Ag/ZrO_2 and Ag/MgO, with a maximum at ca. 300 °C; Ag/SiO_2 and Ag/TiO_2, with selectivity exceeding 80% at 350 °C; and Ag/Al_2O_3 and Ag-ZSM-5, with relatively low selectivity below 400 °C. For Ag/SiO_2 and Ag/TiO_2, the decrease in N_2 selectivity above 350 °C was due to the increase in NO_x formation. The relatively low N_2 selectivity of Ag/Al_2O_3 was due to significant formation of NH_3, reaching a maximum selectivity to NH_3 of 70% at 450 °C.

The ACN conversions and N_2 selectivity over Ag supported on various materials in the presence of H_2O are presented in figure 3. Over Ag/ZrO_2 and Ag/MgO, the ACN conversions were slightly increased in the presence of H_2O (figure 3a). Over Ag/SiO_2, the presence of H_2O resulted in a drastic increase in the ACN conversion at 250 °C. The ACN conversions over Ag/TiO_2 and Ag-ZSM-5 were also slightly increased in the presence of H_2O, but the ACN conversion over Ag/Al_2O_3 decreased. Over Ag/ZrO_2 and Ag/TiO_2, the presence of H_2O resulted in an increase in N_2 selectivities at 250 and 300 °C, respectively. The N_2 selectivities over Ag/ZrO_2 decreased above 400 °C, due to the increase in NO_x formation. Over Ag/SiO_2, N_2 formation at 250–350 °C was suppressed, with significant formation of NH_3 instead. Over Ag/MgO, N_2 formation was also suppressed, with formation of more NO_x. Over Ag/Al_2O_3 and Ag-ZSM-5, the N_2 formation decreased further, resulting in an increase in NH_3 and NCPs, respectively. These results suggest that ZrO_2, SiO_2, and TiO_2 are the preferred supports for Ag and that addition of H_2O to the feed gas enhances the activity of these catalysts for ACN decomposition.

NH_3 was formed with almost all of the catalysts, both in the presence and absence of H_2O. We speculate that NH_3 is formed through hydrolysis of ACN. The fact that NH_3 was formed over Ag/SiO_2 suggests that Ag has hydrolysis activity since SiO_2 has negligible activity, as already mentioned.

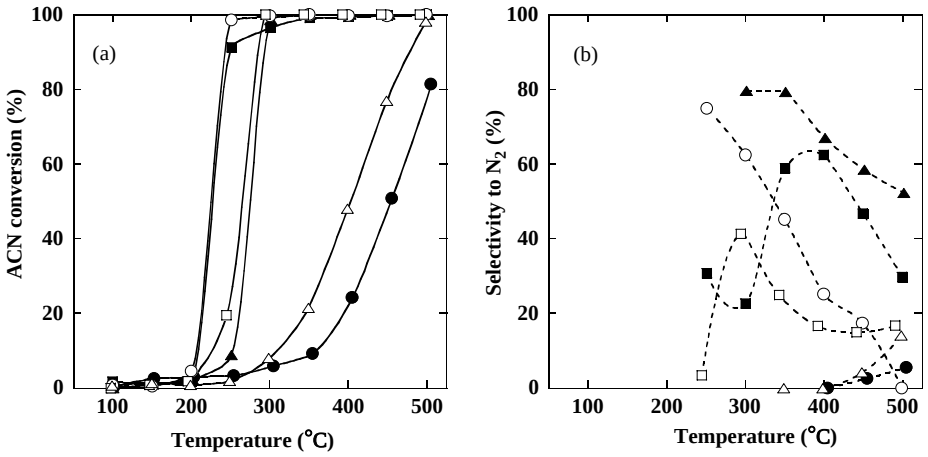

Figure 3. ACN conversion (a) and selectivity to N_2 (b) over Ag catalysts supported on various materials. $W/F = 0.0375$ g s/cm^3. The feed gas consisted of ca. 200 ppm ACN, 5% O_2, and 0.5% H_2O. Symbols indicate Al_2O_3 (●), SiO_2 (■), TiO_2 (▲), ZrO_2 (○), MgO (□), and ZSM-5 (△).

To clarify the role of NH_3 in the N_2 formation step, NH_3 oxidation reactions were carried out in the presence of 0.5% H_2O over Ag/SiO_2, Ag/TiO_2, and Ag/ZrO_2 (figure 4). The order of the activity for NH_3 oxidation was $Ag/ZrO_2 > Ag/TiO_2 > Ag/SiO_2$. The N_2 selectivities were similar to those obtained in the ACN decomposition reaction (figure 3). These results support our speculation that N_2 formation during ACN decomposition proceeds through oxidation of NH_3. To improve the N_2 selectivity in ACN decomposition over Ag catalysts, it is necessary to further clarify the role of NH_3 as an intermediate and the role of the support in the reaction of NH_3.

3.3. Cu catalysts

The ACN conversions and N_2 selectivity for the ACN + O_2 reaction over Cu supported on five kinds of metal oxides and Cu-ZSM-5 are presented in figure 5. The ACN conversion depended on the support material, the order being $TiO_2 > ZrO_2 >$ ZSM-5 $= Al_2O_3 >$ MgO $> SiO_2$ (figure 5a). The N_2 selectivities were also influenced by the support material (figure 5b). Cu-ZSM-5 had the highest N_2 selectivity (ca. 80% over 300 °C), followed by Cu/Al_2O_3. Although Cu/TiO_2 and Cu/ZrO_2 can decompose ACN around 200 °C, the N_2 selectivity achieved with these catalysts was at most 70%, and the temperature range for high N_2 yield was narrower than with Cu-ZSM-5. The decrease in N_2 selectivity at higher temperatures for Cu catalysts supported on metal oxide was due to an increase in NO_x formation.

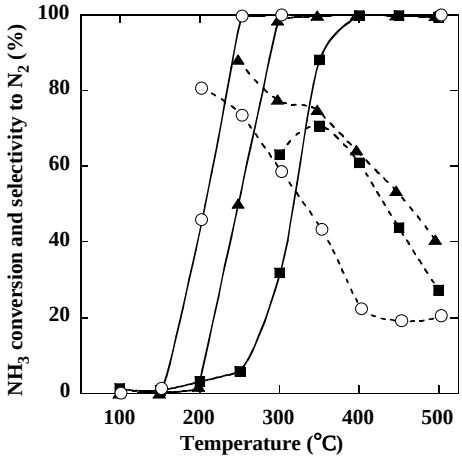

Figure 4. NH_3 conversion (solid lines) and selectivity to N_2 (broken lines) over Ag/SiO_2 (■), Ag/TiO_2 (▲), and Ag/ZrO_2 (○). $W/F = 0.0375$ g s/cm^3. The feed gas consisted of ca. 300 ppm NH_3, 5% O_2, and 0.5% H_2O.

The ACN conversions and N_2 selectivity for the ACN + O_2 + H_2O reaction over Cu supported on various materials are presented in figure 6. Over Cu/ZrO_2 and Cu/SiO_2, the ACN conversions were slightly decreased by the addition of H_2O. Moreover, N_2 selectivities of all of the metal oxide supported Cu catalysts were drastically suppressed. Cu-ZSM-5, however, showed no change in ACN conversion and N_2 selectivity, the latter increasing in the presence of H_2O. A certain amount of HCN and a small amount of NH_3 were formed at 250 °C. The decrease in the N_2 selectivity over Cu/Al_2O_3, Cu/TiO_2, and Cu/ZrO_2 was accompanied by increases in NH_3 and NO_x formation, and, for Cu/SiO_2 and Cu/MgO, NH_3 was formed. We conclude that Cu-ZSM-5 has the most appropriate activity among the Cu catalysts investigated.

Since NH_3 is formed over Cu/SiO_2, Cu itself, like Ag, has activity for hydrolysis. NH_3 oxidation in the presence of H_2O over Cu-ZSM-5 and Cu/Al_2O_3 was carried out, the results being shown in figure 7. For Cu-ZSM-5, the NH_3 conversion trend was similar to that for ACN conversion, and the N_2 selectivity was quite high. For Cu/Al_2O_3, the N_2 selectivity was similar to that for ACN decomposition above 400 °C. From these results, ACN decomposition is thought to proceed

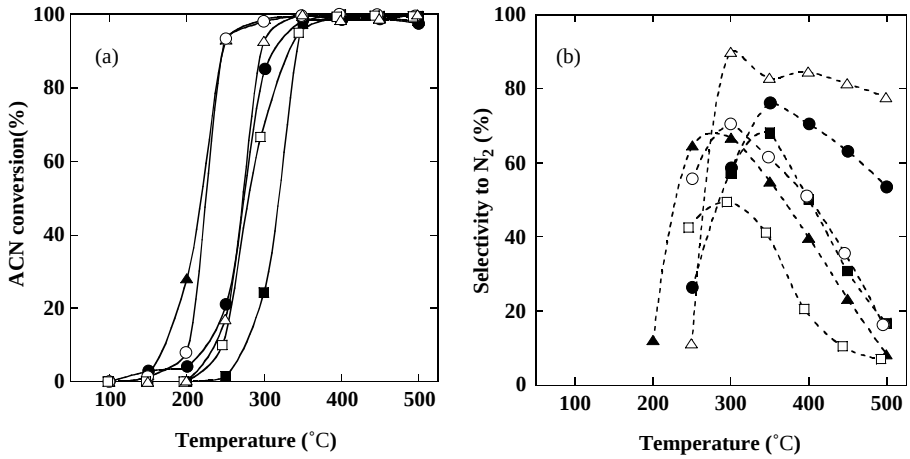

Figure 5. ACN conversion (a) and selectivity to N_2 (b) over Cu catalysts supported on various materials. $W/F = 0.0375$ gs/cm^3. The feed gas consisted of ca. 200 ppm ACN and 5% O_2. Symbols indicate Al_2O_3 (●), SiO_2 (■), TiO_2 (▲), ZrO_2 (○), MgO (□), and ZSM-5 (△).

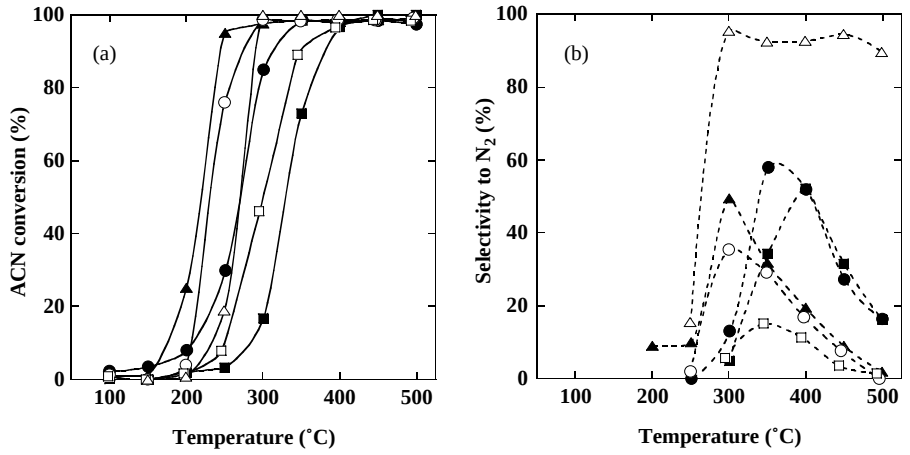

Figure 6. ACN conversion (a) and selectivity to N_2 (b) over Cu catalysts supported on various materials. $W/F = 0.0375$ g s/cm^3. The feed gas consisted of ca. 200 ppm ACN, 5% O_2, and 0.5% H_2O. Symbols indicate Al_2O_3 (●), SiO_2 (■), TiO_2 (▲), ZrO_2 (○), MgO (□), and ZSM-5 (△).

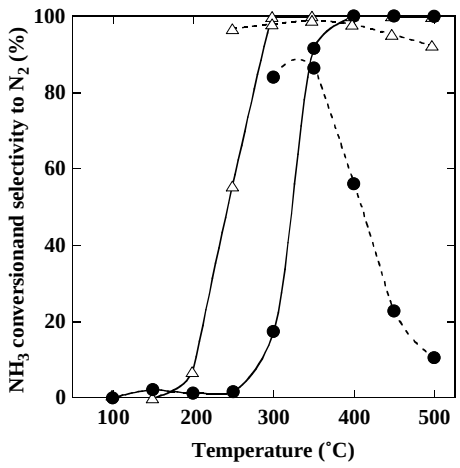

Figure 7. NH_3 conversion (solid lines) and selectivity to N_2 (broken lines) over Cu-ZSM-5 (△) and Cu/Al_2O_3 (●). $W/F = 0.0375$ g s/cm^3. The feed gas consisted of ca. 300 ppm NH_3, 5% O_2, and 0.5% H_2O.

mainly through NH_3 formation and oxidation over these catalysts, too. With Cu-ZSM-5, however, we also detected HCN, which was suggested to decompose to N_2 [6]. Thus further study is needed to clarify the reaction mechanism.

The activities of ACN decomposition over the support materials without Cu were lower than those over the Cu-supported catalysts, both in the presence and absence of H_2O. Clearly, Cu is an essential component for ACN decomposition. To clarify the promotional effect of the ZSM-5 support, we carried out NH_3-TPD for each support and Cu catalyst. Figure 8a shows NH_3 desorption profiles for the Cu catalysts. Cu-ZSM-5 exhibited not only the largest uptake of NH_3 but also the highest NH_3 desorption temperature, at 600 °C. Cu/Al_2O_3 exhibited a larger uptake than other Cu-supported metal oxides. For Cu/Al_2O_3, Cu/SiO_2, Cu/TiO_2, and Cu/ZrO_2, the NH_3 uptake values were larger than those for the corresponding support materials. For Cu-

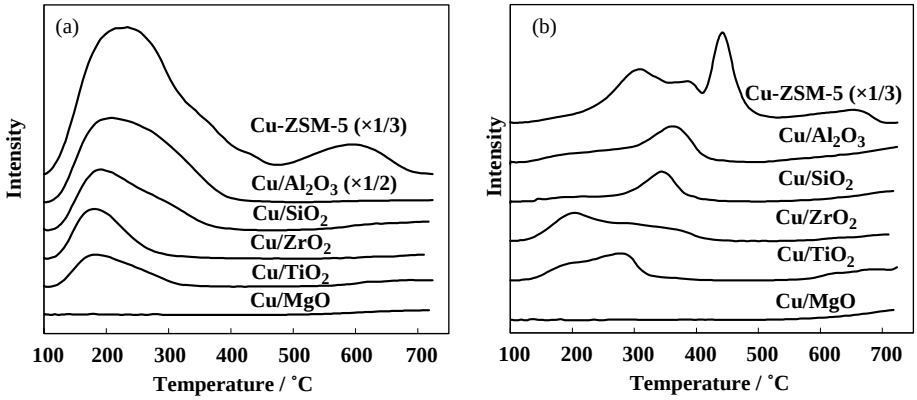

Figure 8. NH_3 and N_2 evolution during NH_3-TPD of Cu catalysts.

ZSM-5, the NH_3 desorption temperatures became higher than that for H-ZSM-5. It is suggested that Cu on these supports becomes an adsorption site for NH_3. Figure 8b shows N_2 evolution in the NH_3-TPD experiments. All the Cu catalysts except for Cu/MgO exhibited N_2 evolution, accompanying H_2O formation. This result suggests that lattice oxygen was consumed and that part of the Cu was reduced. Three N_2-formation peaks were observed for Cu-ZSM-5, and the total amount of N_2 evolution was much larger than for other catalysts. It is supposed that ZSM-5 forms certain Cu species that strongly adsorb NH_3 and produce N_2 through the decomposition of NH_3.

Figure 9 shows XRD patterns of Cu catalysts. The diffraction peak for bulk CuO was observed on Cu-ZSM-5, Cu/SiO_2, Cu/TiO_2, and Cu/MgO. Cu/Al_2O_3 and Cu/ZrO_2, however, had no peak attributed to this Cu species.

The H_2-TPR profiles of the Cu catalysts are presented in figure 10. Cu-ZSM-5 exhibited peaks at 270 and 400 °C. The peak at 270 °C, which has a shoulder at around 240 °C, probably corresponds to the reduction of isolated Cu^{2+} to Cu^+ and of CuO aggregates to Cu^0, and the peak at 400 °C corresponds to the reduction of Cu^+ to Cu^0 [7]. It is suggested that Cu-ZSM-5 contained both dispersed Cu^{2+} ions and bulk CuO species after preparation. Cu/Al_2O_3 exhibited only one peak, at 230 °C, which may be attributed to isolated Cu^{2+} ions or finely dispersed CuO [8–10]. Cu/TiO_2 and Cu/ZrO_2 had reduction peaks at around 150 °C. Such H_2 consumption below 200 °C is ascribed to the reduction of Cu^{2+} ions [11,12]. The peak at 260 °C for Cu/ZrO_2 suggests finely dispersed CuO, since the XRD pattern for this sample exhibited no diffraction peak attributed to CuO. Cu/SiO_2 and Cu/MgO exhibited only one peak, at around 280 °C, attributed to CuO reduction. The H_2/Cu ratios for Cu/SiO_2, Cu/TiO_2, Cu/ZrO_2, and Cu/MgO in the TPR were roughly unity, which indicates that below 350 °C, Cu in the oxidized state can be reduced by H_2 to a metallic state on these catalysts. By contrast, the ratio for Cu/Al_2O_3 was only 0.66, which indicates

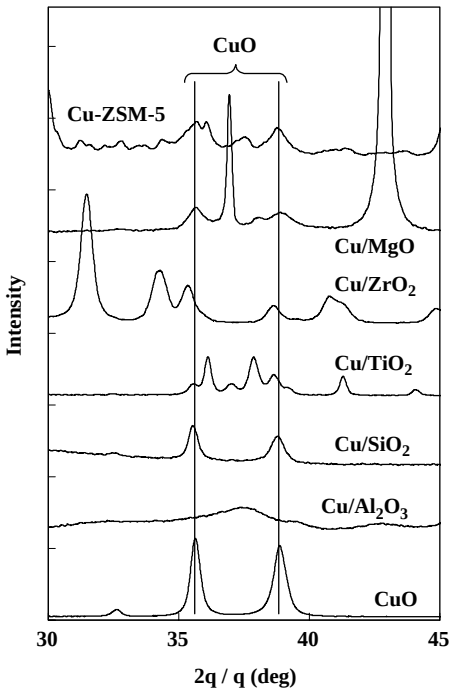

Figure 9. XRD profiles of Cu catalysts.

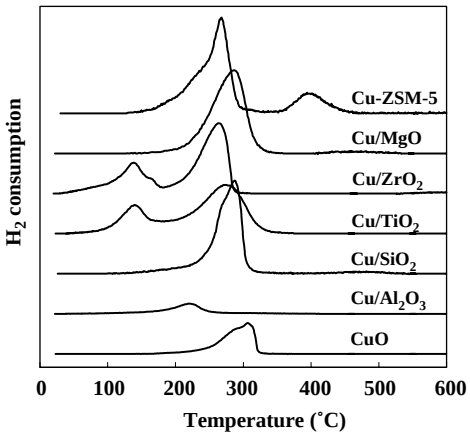

Figure 10. H_2-TPR profiles of Cu supported on various materials.

unreduced Cu^+ ions may persist on Al_2O_3 until the highest temperature applied. Cu Al_2O_3 is known to maintain Cu^+ state after H_2 reduction [13,14].

Cu-ZSM-5 and Cu/Al_2O_3 have a high NH_3 adsorption capacity and maintain Cu^+ ions in the presence of H_2 even at high temperatures. Cu^+ species may be involved in the high N_2 selectivity. The Cu species in ZSM-5 are known to be located in cation positions, and those in Al_2O_3 are located in the octahedral and tetrahedral coordination sites [8]. Although the initial states of the Cu species in ZSM-5 and Al_2O_3 may be different, it is thought that the ability of the support to maintain Cu^+ ions is important. Note that the area of the higher reduction peak ascribed to Cu^+ ions in ZSM-5 was independent of the co-existence of H_2O during the pretreatment and TPR measurement. The result accounts for the fact that Cu-ZSM-5 retained high N_2 selectivities in the presence of H_2O.

4. Summary

Catalysts for decomposing ACN with a high N_2 selectivity were explored. Both Cu and Ag showed high N_2 selectivity and ACN conversion. The presence of H_2O promotes ACN decomposition over Ag catalysts. Cu-ZSM-5 exhibited the highest N_2 selectivity >80% above 350 °C, and was concluded to be the most promising catalyst for ACN decomposition.

References

[1] S.P. Felter and J.S. Dollarhide, Regul. Toxicol. Pharmacol. 26 (1997) 281.
[2] D.R. van der Vaart, W.M. Vatvuk and A.H. Wehe, J. Air Waste Manage. Assoc. 41 (1991) 92.
[3] A. Gervasini and V. Ragaini, Catal. Today 60 (2000) 129.
[4] S. Akaratiwa, T. Nanba, A. Obuchi, J. Okayasu, J.-Oi. Uchisawa and S. Kushiyama, Top Catal. 16/17 (2001) 209.
[5] T. Nanba, A. Obuchi, Y. Sugiura, C. Kouno, J. Uchisawa and S. Kushiyama, J. Catal. 211 (2002) 53.
[6] I.O.Y. Liu and N.W. Cant, J. Catal. 195 (2000) 352.
[7] G. Delahay, B. Coq and L. Broussous, Appl. Catal. B 12 (1997) 49.
[8] G. Centi and S. Perathoner, Appl. Catal. A 132 (1995) 179.
[9] G. Centi, S. Perathoner, D. Biglino and E. Giamello, J. Catal. 152 (1995) 75.
[10] R.M. Friedman and J.J. Freeman, J. Catal. 55 (1978) 10.
[11] R.-X. Zhou, T.-M. Yu, X.-Y. Jiang, F. Chen and X.-M. Zheng, Appl. Surf. Sci. 148 (1999) 263.
[12] F. Boccuzzi, A. Chiorino, G. Martra, M. Gargano, N. Ravasio and B. Carrozzini, J. Catal. 165 (1997) 129.
[13] L. Chen, T. Horiuchi, T. Osaki and T. Mori, Appl. Catal. B 23 (1999) 259.
[14] R. Hierl, H. Knözinger and H.-P. Urbach, J. Catal. 69 (1981) 475.